Human Heart Blood Flow Simulations Based on CFD

Dean Vucinic[1], Tao Yang[1,2], Andrey A. Aksenov[3]

[1]Vrije Universiteit Brussel, Belgium
[12]Xi'an Modern Control Technology Institute, China
[3]Capvidia/TESIS, Moscow, Russia

Received [**23rd February2015]**; Revised [**9th April 2015**]; Accepted [**21st June 2016**]

Abstract: **In this paper, the modeling and simulation of the blood flow in the real patient heart is described. In order to cure the patients with cardio vascular disorder it is important to make appropriate choice of an artificial heart valve, it is important to exactly understand the behavior of the heart blood flow of the specific patient under treatment. The presented approach is based on the Magnetic Resonance Imaging/Tomography, which provides the necessary input to create the heart shape ("its geometry") and its variation in time (tens or hundreds of frames) to define the internal time-dependent heart volumes for one heartbeat. Once this geometry is defined, the CFD software is applied to simulate the internal blood flow and further on visualize it to enable its further analysis. The applied CFD tool is FlowVision, due to its possibility to fully automatically perform the mesh generation of arbitrary shapes, as the heart geometry requires. In addition, FlowVision applies the dynamic mesh refinement by taking into account the motion of the heart-modeled surface, required by the CFD Euler model. The presented CFD approach to simulate the human internal blood flow is validated with data from MRI/MRT scans of the real heart and the respective simulation test cases are presented.**

Keywords: **human heart,MRI/MRT, internal flow CFD simulation, time-variant geometry,boundary conditions.**

I. INTRODUCTION

Today, CVDs (Cardio Vascular Disorder) are the first cause of death. By 2030, CVD-related deaths will reach 23.3 million each year [1]. The lack of realistic human models limits ability to predict device behaviour under realistic use conditions. Ultimately, 95% of all new devices are not tested in a human environment before approval. The growth in recalls suggests room for improvements.

The numerical simulation method, for the modellingthe human heart flow, makes feasible to design or test an artificial medical device for substitution, through this more efficient and low-cost approach. Moreover, with the presented approach we can deeply study the heart functioning under different, even abnormal conditions, and to visualize the internal flow field behaviour of the heart motion in a more convenient way.

One heart cycle contains 2 phases: (1) diastole (ventricle filling) and (2) systole (ventricle contraction). It is well known that atriumis filled with fresh blood. During the diastole phase, the atria and ventricles of the heart relax and begin to fill with blood. Then, the atria begin to relax. In the next phase, the heart's ventricles contract (ventricular systole) and the blood is pump out from the heart. At the end of diastole, the heart's atria contract (atrial systole) and pump the blood into the ventricles. A heartbeat may be considered asthe simple, periodically repeated event. However, it involves the complex series of very precise and coordinated events, which take place inside and around the heart.

A typical heartbeat cycle is shown in Figure 1. It can be noticed that its shape and volume always keep changing during the heartbeat cycle. This brings new challenges to the CFD modelling and simulation, which are difficult to be solved with the traditional numerical methods, and these challenges are (1) the time-variant shape of the heart geometry having big deformations and requiring high-quality mesh deformation detection for its remeshing; (2) the boundary conditions are changing in time, and from Wiggers Diagram (a standard diagram used in cardiac physiology) we can extract the BC for the inlet or outlet; (3) the complex heart geometry has plenty of tiny features, which capturing needs a very fine mesh creation in order to guarantee the robustness for the applied numerical scheme.

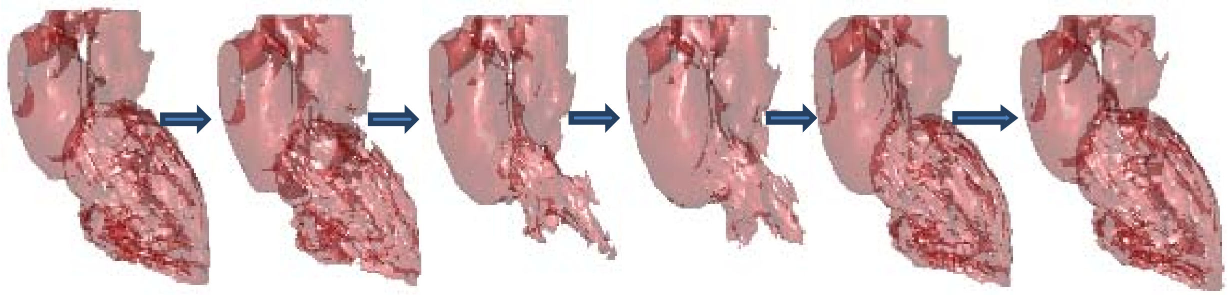

Figure 1 The heart model time-dependent shape during the heartbeat cycle

In recent years, the Computational Fluid Dynamics (CFD) simulation of the heart flow has made great progress and has been playing an important role in investigating the heart functionality. The most active CFD approaches to simulate the heart flow might be roughly classified in 3 types: (1) geometry-prescribed CFD methods, (2) fictitious Fluid-Structure Interaction (FSI) methods and (3) realistic FSI methods [5]. The geometry-applied in CFD, for modelling the moving meshes or boundaries is constructed mostly from Computerized Tomography (CT) or Magnetic Resonance Imaging/Tomography (MRI/MRT) data [6]–[9]. However, almost all of them need to undergo some simplifications, when creating the heart geometry for simulating the heartbeat process.

In this paper, a dynamically adaptive grid method, based on the moving body feature available in FlowVision is described. This is combined with the automatic geometry replacement, enabling the dynamic simulation of the heartbeat process and the thus modelling the internal flow mechanism of the human heart.

II. NUMERICAL MODELLING

The applied numerical schemes are integrated in the FlowVision software, which is based on the Cartesian grid when solving the URANS equations. An important feature is the dynamic mesh adaptation, which is automatically performed to reconstruct dynamically the mesh in real-time. This is especially interesting when adapted to the dynamic geometry of the heartbeat, where the solver automatically replaces the changed geometry at each time-variation of the heart shape.

A. Heart frames modelling

The heart model is a dynamic high-fidelity model of a normal (healthy), 4-chamber adult male human heart. It includes well-defined anatomic details of the heart, as well as proximal vasculature, such as the aortic arch, pulmonary artery, and superior vena cava (SVC). By assuming the duration of a heartbeat cycle of 1s, which corresponds to a heart rate of 60 beats per minute, as a typical adult (resting) heart rate.

The heart geometry frames are originated from the DICOM file, which was obtained from the CT scan. By inserting the set of DICOM files in 3D Slicer (100 DICOM files for 1 frame), the heart frames have been generated, as shown in Figure 2.

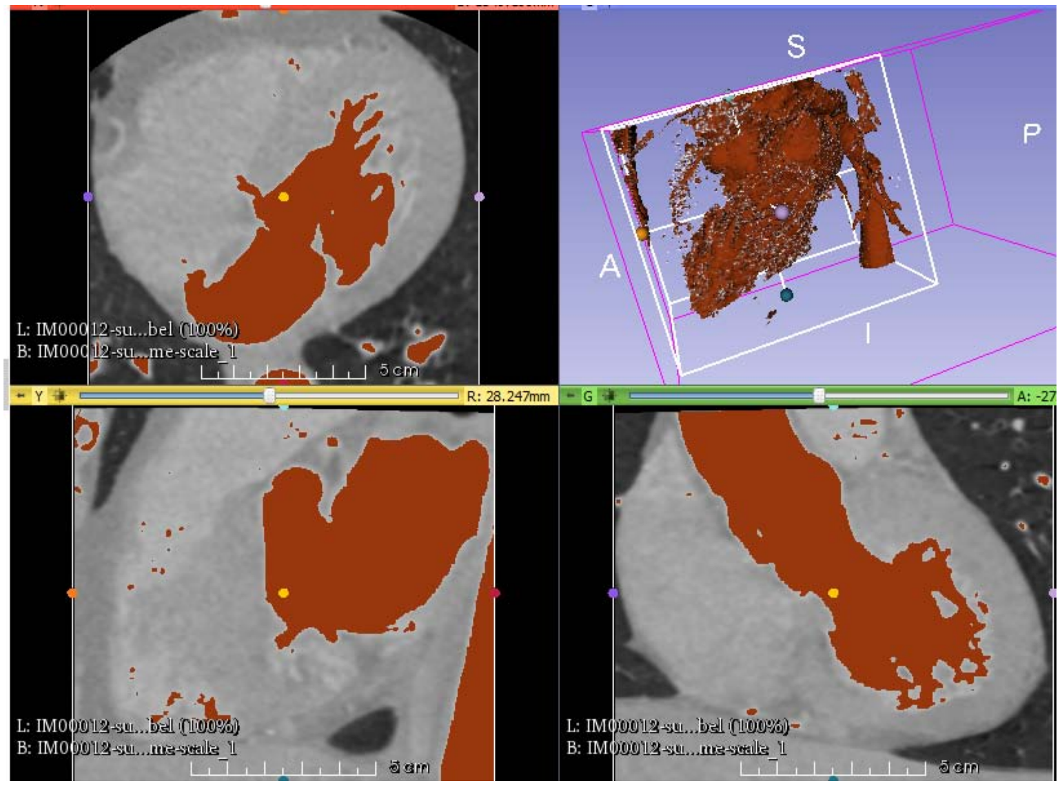

Figure 2 Heart frames generation from CT scan

However, the obtained geometries are still not usable for the CFD simulation tools, since the shape of the heart is very complex and includes many tiny features, which could possibly cause some problems during the required mesh generation. Thus, it is essential to clean and fix the geometries before the CFD modelling is done, and for our specific approach, to be usable in FlowVision. By using these frames, the heartbeat process can be extracted, discretized and simulated in the time dependent way.

B. Governing equations

Numerical simulation of blood flow in heart is based on solution full Navier-Stokes equations for modelling the incompressible fluid flows, governed by the continuity equation:

$$\vec{\nabla} \cdot V = 0$$

The momentum conservation equation is defined as:

$$\rho\left(\frac{\partial V}{\partial t} + \left(V \cdot \vec{\nabla}\right)V\right) = -\vec{\nabla}P + \vec{\nabla}2(\mu + \mu_t)\hat{e}$$

$$\hat{e} = \{e_{ij}\},\ \ e_{ij} = \frac{1}{2}\left(\frac{\partial V_i}{\partial x_j} + \frac{\partial V_j}{\partial x_i}\right)$$

Where t is time, $\rho, V, P, \mu$are respectively density, velocity, pressure, and viscosity of the blood. The blood flow within heart has the high Reynolds number, and we apply the k-ε turbulence model [11] to define μ_t - “turbulent” viscosity parameter in the Navier-Stokes equation:

$$\frac{\partial k}{\partial t} + \vec{\nabla}(Vk) = \frac{1}{\rho}\vec{\nabla}\left(\left(\mu + \frac{\mu_t}{\sigma_t}\right)\vec{\nabla}k\right) + \frac{G}{\rho} - \varepsilon$$

$$\frac{\partial \varepsilon}{\partial t} + \vec{\nabla}(V\varepsilon) = \frac{1}{\rho}\vec{\nabla}\left(\left(\mu + \frac{\mu_t}{\sigma_\varepsilon}\right)\nabla\varepsilon\right) + \frac{\varepsilon}{k}\left(C_1\frac{G}{\rho} - C_2\varepsilon\right)$$

$$G = \mu_t S;\ \mu_t = C_\mu \rho \frac{k^2}{\varepsilon}$$

$$S = \frac{\partial V_i}{\partial x_j}\left\{\mu_t\left(\frac{\partial V_i}{\partial x_j} + \frac{\partial V_j}{\partial x_i}\right)\right\}$$

$$\sigma_k = 1.0, \sigma_k = 1.3, C_\mu = 0.09, C_1 = 1.44, C_2 = 1.92$$

where k is turbulent energy, ε is turbulent energy dissipation.

In addition, the surface boundaries and the boundary conditions need to be carefully defined as shown in Figure 3.

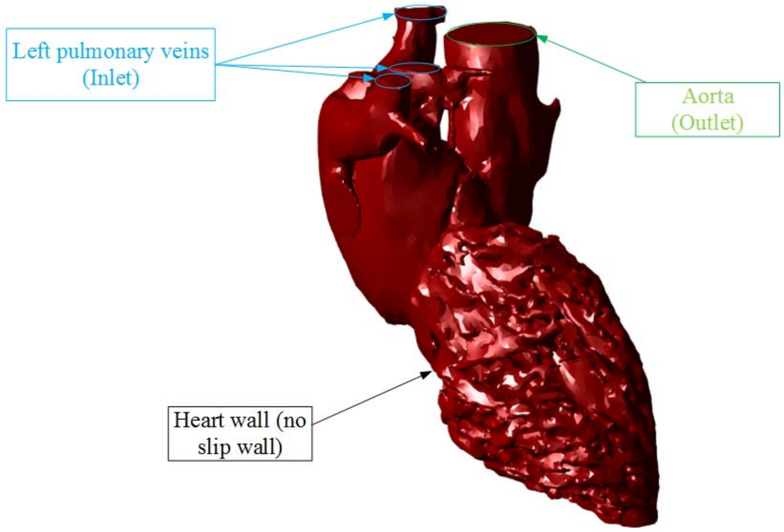

Figure 3 Boundaries of heart frame

C. Dynamic mesh adaptation

The living heart has a very complex surface, which requires a special treatment to be used for the ordinary CFD modelling and simulation process, due to the motion of the heart walls, which require the generation of curvilinear meshes, with use of the Lagrange approach. The FlowVision software has a very interesting functionality as it has a fully automatized mesh generator procedure based on the sub-grid geometry resolution method (SGGR) [12]. SGGR is advanced analogy of the well-known cut-cell method. In SGGR, the initial Cartesian mesh is introduced in the computational domain, and then the mesh cells are intersected by the heart surface boundaries within the computational domain, where the intercepted cut cells containing the heart surface are transformed into complex polyhedrons. In order to take into account the motion of the heart walls, the Euler approach is applied. In this approach the walls are moving along the stationary mesh, and in this process the mesh cells could be: created, deleted and possibly undergo the change of their shape and volumes. All the governing equations are approximated on the basis of this applied mesh, which cell volumes, are allowed to change in order to take into account the geometry change imposed by the moving walls, which directly affect the blood flow characteristics. The mesh is refined (adapted) by using the 2 conditions: (1) to resolve the fine structures of the heart surface, and (2) to resolve high gradients of the blood flow velocity, in order to achieve the sufficient accuracy of the numerical simulations. The mesh adaptation results, which are coming from splitting the mesh cell into 8 smaller cells is modelled as an octree of cells in the computer memory. The blood flow is assumed to be non-stationary, and during the simulation the conditions for the mesh refinement might not be satisfied in some specific regions. In this case, the reverse process of making the mesh coarser is applied: where the previously refined cells are joined together to form a bigger cell, and in this way a fully dynamic mesh adaptation is achieved.

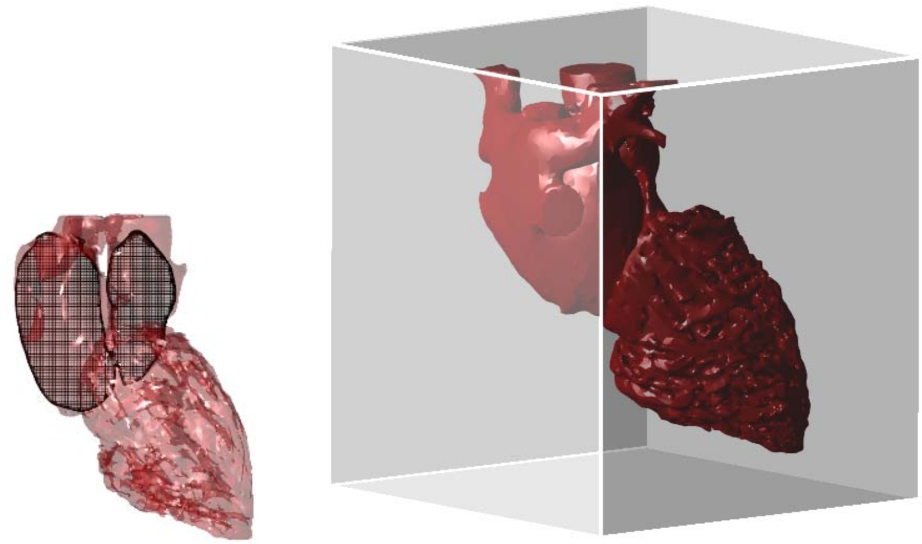

Figure 4 Cuboid for initial mesh generation

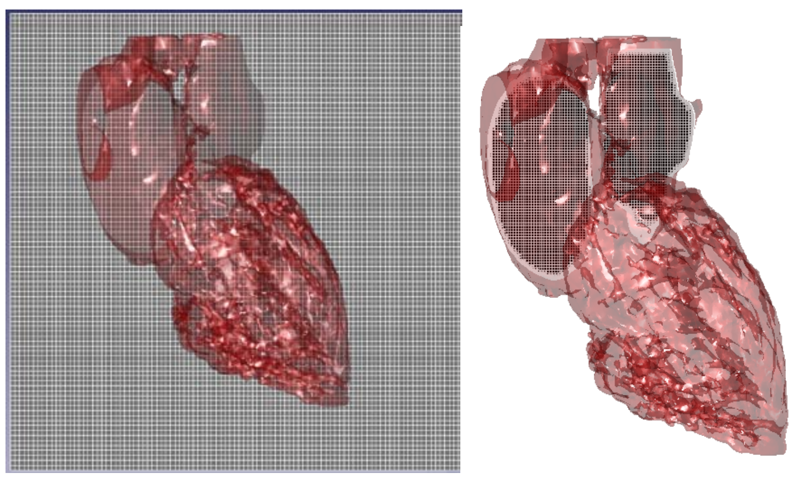

Figure 5 Mesh applied for heartbeat simulation

The dynamic mesh adaptation can be possibility used for the mesh convergence independence tests. The blood flow simulation during the heart beating is made under the several mesh adaptation criteria in order to calculate the dependency of the mesh refinement parameters. Such dependency criterion is used when the coarsest mesh can be substitute with the fine mesh by not affecting the simulation, and such process is presented in this paper.

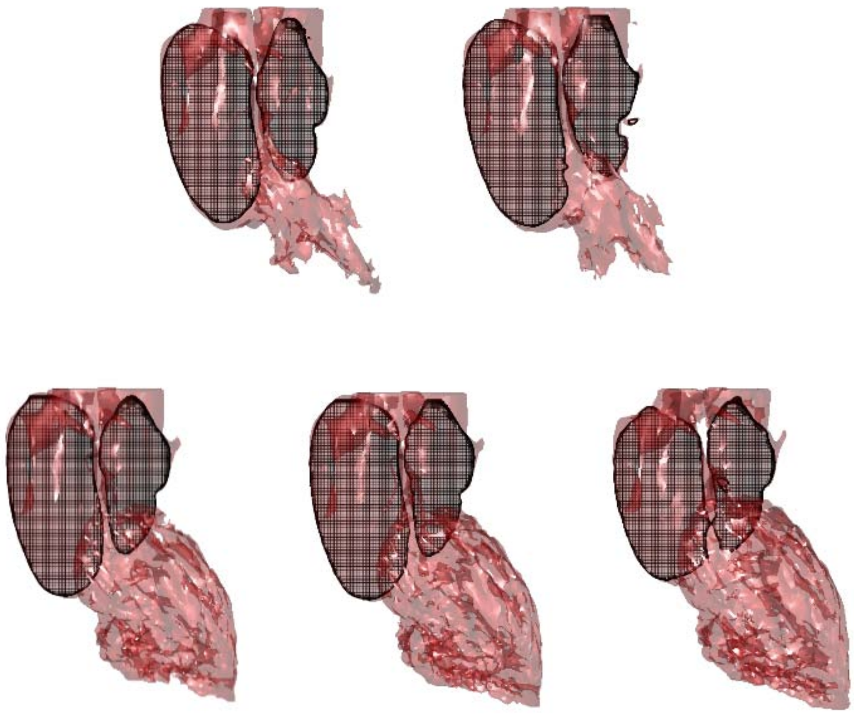

Figure 6 Mesh deformation within heartbeat process

Since it is an internal flow problem and the shape of heart is irregular, at the beginning, a cuboid (Figure 4) is introduced to create the initial Cartesian mesh. The initial number of cells, respectively in X, Y and Z direction are 90, 83, and 92. The 2 planes are created for the inlet and the outlet boundaries, which are combined to close the heart volume, to form a simply connected domain, as the volume of control. The volume adaption with level number 1 is used to refine the mesh in the computational domain, and the surface adaption with level 3 and 2 cell strata for the heart surface are created, as shown in Figure 5.

The heart shape geometry of the heartbeat process is time dependent, and requires that the mesh is reconstructed dynamically in real-time, thus the total number of cells is dynamic, and changes in time, and for this particular case is ranging from 2.0 to 3.2 million, as shown in Figure 6.

D. Numerical setup

The modelling of the internal flow of the heartbeat cycle, depends on the blood property, which has a big influence on the simulation results. The blood viscosity is determined by plasma viscosity, haematocrit (volume fraction of red blood cell, which constitutes 99.9% of the cellular elements) and mechanical properties of red blood cells. The red blood cells have unique mechanical behaviour, which can be discussed under the terms erythrocyte deformability and erythrocyte aggregation [2]. Because of that, the blood behaves as a non-Newtonian fluid. However, it is reasonable to regard it as a Newtonian fluid, when modelling the arteries with diameters larger than 1 mm [3]. Considering the size of the heart ventricle, as they are much bigger than 1mm, we can use the Newtonian fluid to model the blood flow inside the heart.

The assumed blood viscosity is 0.0035 kg/(m·s) (i.e. 3.5 mPa·s), as shown in Fig. 7. As such, the blood can meet the Newtonian fluid requirement in rheology. The main parameters applied to characterize the blood are summarized in Table I.

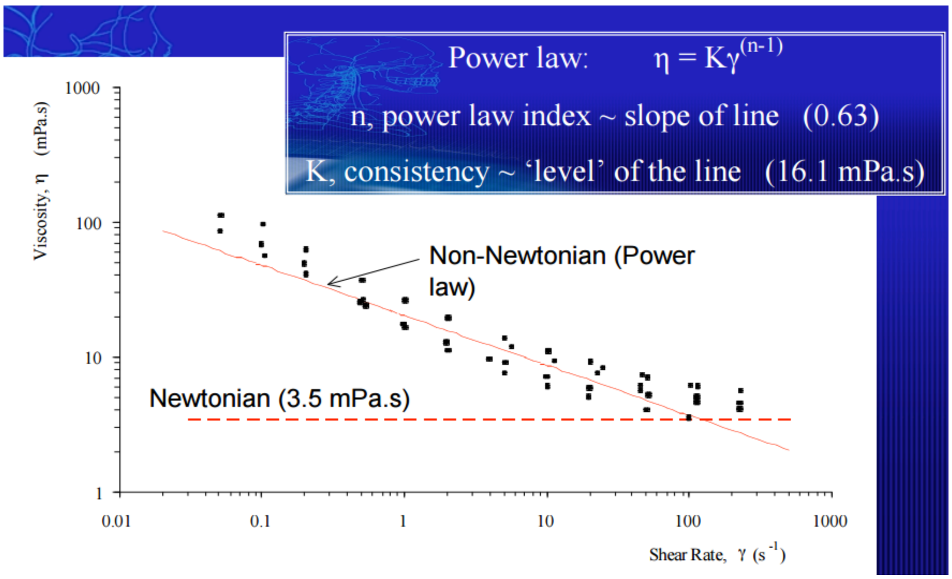

Figure 7 Rheology of Human Blood [2]

TABLE I: PARAMETERS APPLIED FOR BLOOD

Symbol	Physical quantity	Value
μ	viscosity	0.0035 kg/(m·s)
ρ	density	1035 kg/m^3
Cp	specific heat	3470 J/(kg·K)

TABLE II: NUMERICAL SETUP APPLIED IN FLOWVISION

Numerical setup	Quantity	Value
Inlet	Type Normal mass velocity	Inlet Time-variant, kg / (m2 ·s)
Outlet	Type Pressure	Outlet Time-variant, Pa
Initial flow field	Velocity Pressure	0 m/s 10666 Pa
Physical Processes	Heat Transfer Turbulence Model	None KES (standard k-ε model)
Numerical Scheme	Implicit/Explicit Time Step	Implicit new 0.001 s

The numerical setup applied in FlowVision is listed in Table II. The URANS equations are solved in order to simulate the heartbeat process. The flow medium is blood and modelled under the low speed internal flow regime. In such case, it is reasonable to assume that the flow is incompressible and without the heat transfer. For simulating the turbulence, the KES model (standard k-ε turbulence model) has been applied. In the macro-circulation, the blood vessels are relatively large and the fluid velocity is relatively high, and therefore, the standard k-ε turbulence model is commonly used to solve the flow field under these conditions [4].

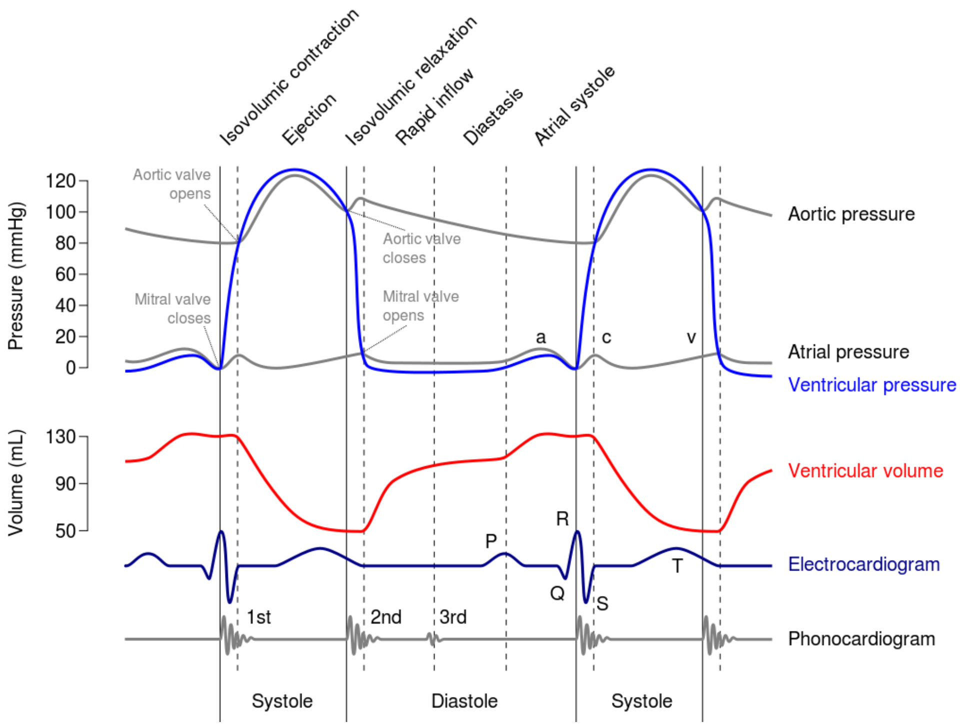

Figure 8 Wiggers diagram

The parameters of the time-dependent boundary conditions are extracted from the Wiggers diagram (Figure 8), which is a standard diagram used in the cardiac physiology. The cardiac cycle is the sequence of events that occurs when the heart beats. There are 2 phases of the cardiac cycle. In the diastole phase, the heart ventricles are relaxed and the heart fills with blood. In the systole phase, the ventricles contract and pump blood to the arteries. One cardiac cycle is completed when the heart fills with blood and the blood is pumped out of the heart.

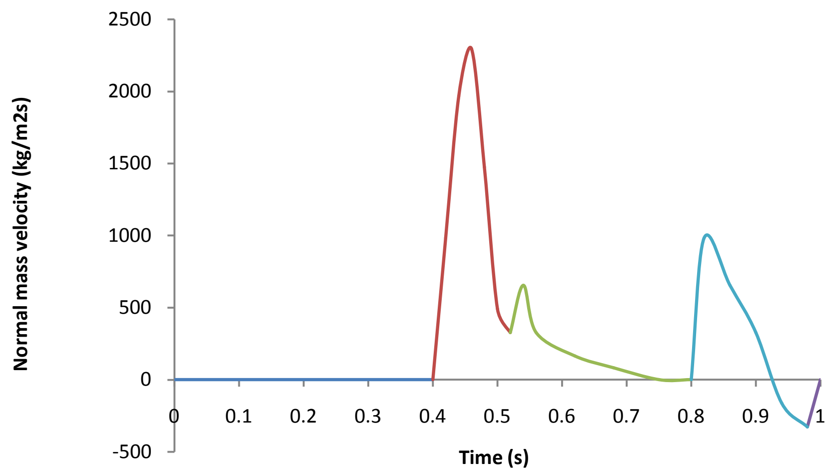

(a) Normal mass velocity of inlet

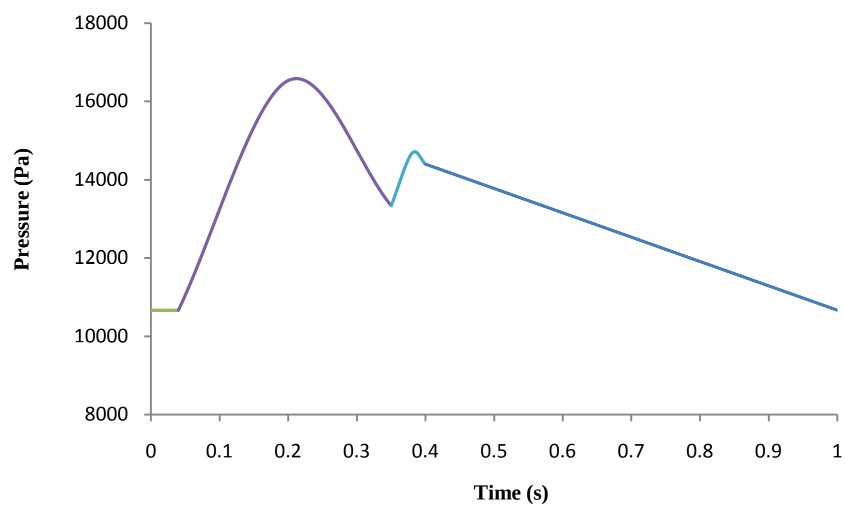

(b) Pressure of outlet

Figure 9 Applied parameters for the boundary conditions

The aortic pressure can be used to define the pressure for outlet (Figure 9(b)) and the normal mass velocity of the inlet can be deduced from the ventricular volume (Figure 9(a)). When modelling this case, we assume the heart beat cycle is 1 sec. Thus, for the normal mass velocity during the systole period there is no inflow for the inlet before 0.4s, so it is equal to 0 kg / ($m^2 \cdot s$). Afterwards, the diastole period starts, the normal mass velocity is not zero, and when combined with the volume rate and the inlet area, the mass velocity of the inlet can be obtained by using the following equation:

$$\dot{m} = \frac{\rho}{S} \cdot \frac{\Delta V}{\Delta t}$$

where $\dot{m}$ is the mass velocity, $\rho$is the density, S is the area of inlet, V is the volume of ventricular and t is the time.

The time-variant boundary conditions should be defined in time, as shown in Figure 9, the curves need to be converted to the piecewise functions, and as such, applied to model the inlet/outlet conditions.

The time independency has been pursed for the unsteady simulation. Consequently, different time steps (0.01s, 0.005s, 0.002s, 0.001s and 0.0005s) have been tested to ensure the time independent results. When the time step is bigger than 0.001s, the simulations are unstable and diverged around T=0.4s (from that moment the inlet mass velocity has significantly changed). For the time step 0.001s and 0.0005s, the simulations are stable and we obtained similar results. By considering the results reliability and computational efficiency, the selected time step is 0.001s.

E. Dynamic simulation with automatic geometry replacement

In order to simulate the heartbeat process, in which the heart shape is time-variant, 100 heart frames at different stage of heartbeat circulation are generated from the CT scan images, and therefore they can take into account even the smallest features of the real human heart. By solving the URANS equations, and replacing the different heart frames at specific time steps, the heartbeat process has been dynamically simulated in the time dependent way.

As the heart frames are too many it is inappropriate to replace their geometries manually. To overcome this problem we implemented a command lines script to support the batch mode execution (Figure 10) in order to achieve the automatic geometry replacement. These command lines, for the100 heart frames to be simulated, one after another, in the chronological order, ensure that the heartbeat process goes smoothly, and in addition, we increase the robustness of the calculation. As it is affected by the large set of geometric data, Figure 11illustrates the mechanism of the unsteady simulation enabling automatic geometry replacement. There are 10 time steps between the intervals of each 2 adjacent frames. Before each frame replacement, this process automatically saves the intermediate results.

```
SS_PROJECTLOAD</Heartbeat/Heartbeat.fvproj><><><>

SS_APPLYNEWGEOMETRY<OBJECT[66]></Heartbeat_Geom/frame1.wrl>
SS_SOLVESTART_EX<0><RI><10>
SS_DO_NOT_DISTURB
              .
              .
              .

SS_APPLYNEWGEOMETRY<OBJECT[66]></Heartbeat_Geom/frame100.wrl>
SS_SOLVESTART_EX<7><RI><10>
SS_DO_NOT_DISTURB

SS_PRJDATASAVE
SS_PROJECTUNLOAD
SS_SHUTDOWNSOLVER
```

Figure 10 Automatic replacement in batch mode

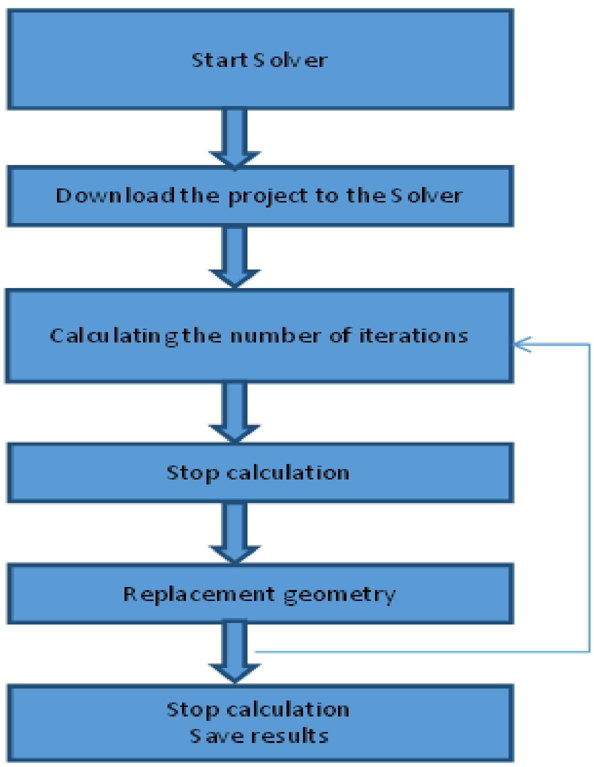

Figure 11 Flow chart of the unsteady simulation

III. RESULTS ANALYSIS

The dynamic simulation was achieved for the heartbeat process (solving one complete heartbeat). Figure 12 shows the convergence history of residuals, and we can notice their fluctuating behaviour in time. Each peak of these curves corresponds to the heart frame replacement. After that, it will soon re-converge, approximately in 10 time steps, and then it will start a new frame replacement cycle.

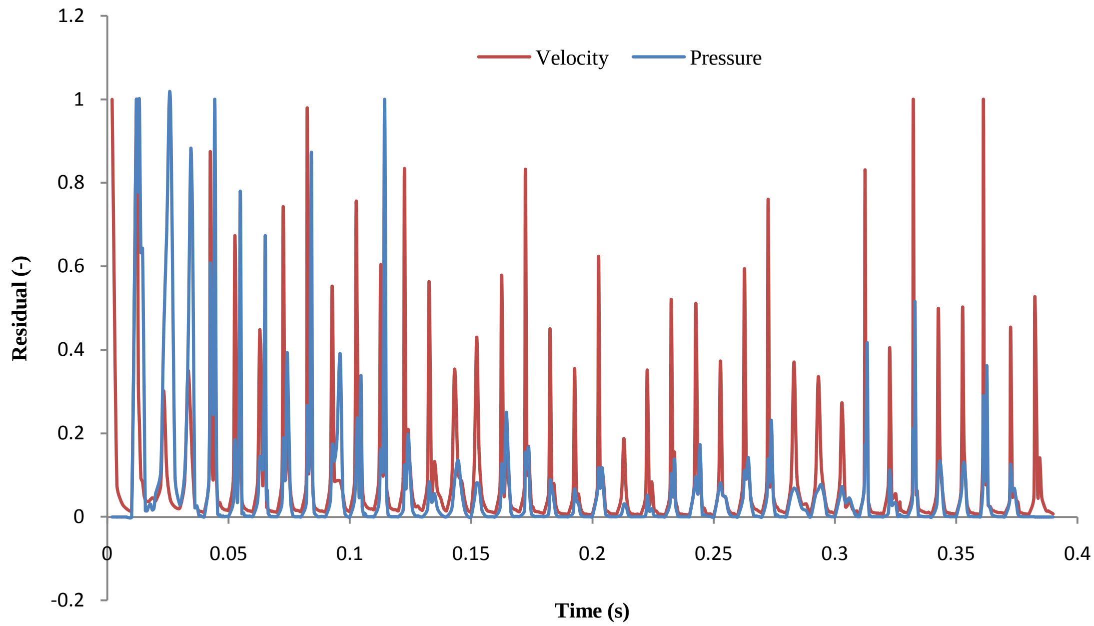

Figure 12 Convergence history of residuals

The dynamic simulation recovers the main characteristics of the real heart internal flow.Figure 13, Figure 14and Figure 15 illustrate the internal flow field state at different times. From a general view, the flow is unsteady and has significant vortex behaviour, which increases the complexity to perform the flow mechanism analysis.

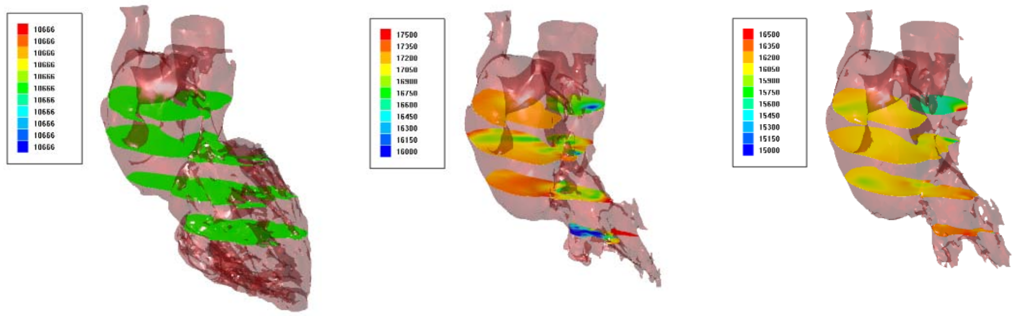

(a) t= 0s (b) t=0.2s (c) t= 0.4s

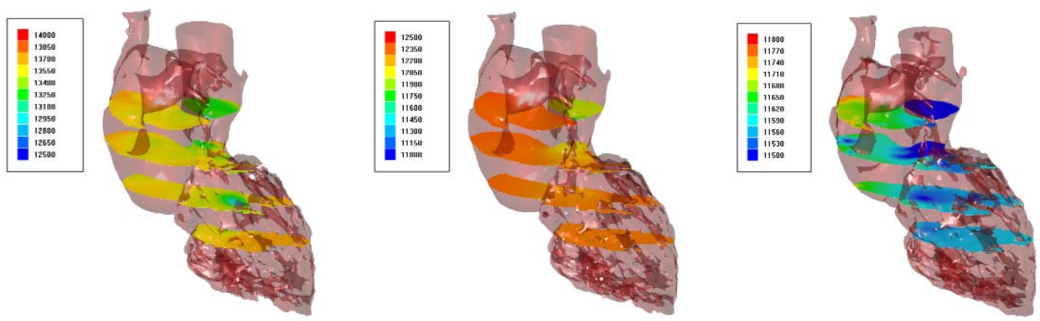

(d) t=0.6s (e) t= 0.8s (f) t=1.0s

Figure 13 Pressure distribution in section planes at different time

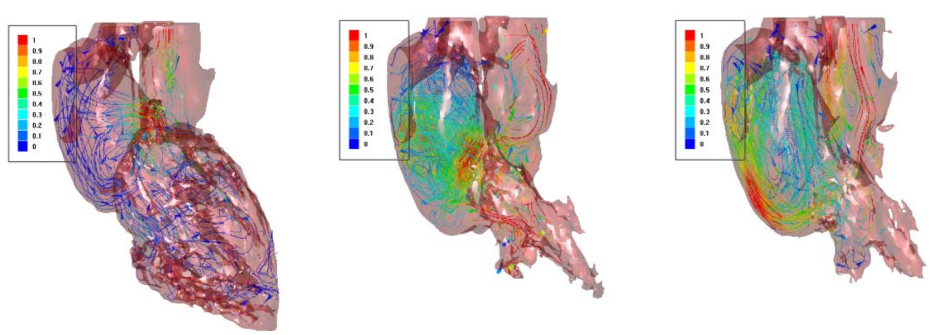

(a) t= 0s (b) t=0.2s (c) t= 0.4s

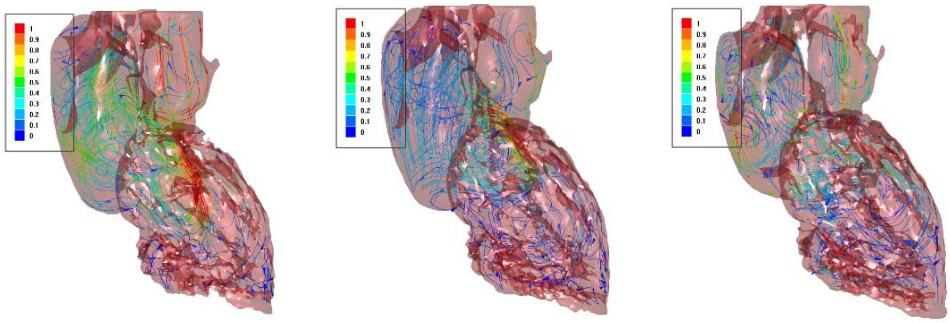

(d) t=0.6s (e) t= 0.8s (f) t=1.0s

Figure 14 3D streamlines inside the heart

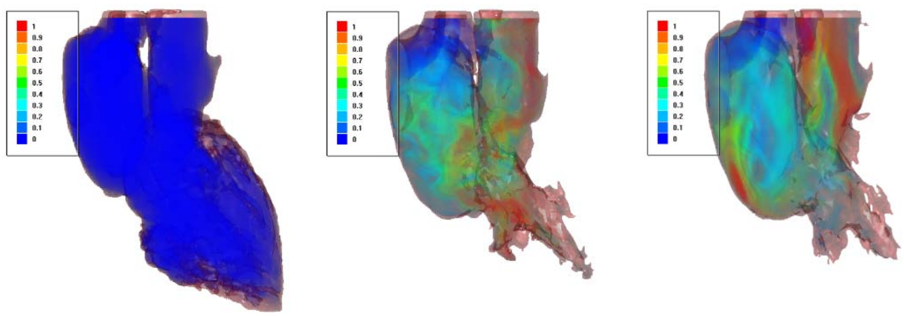

(a) t= 0s (b) t=0.2s (c) t= 0.4s

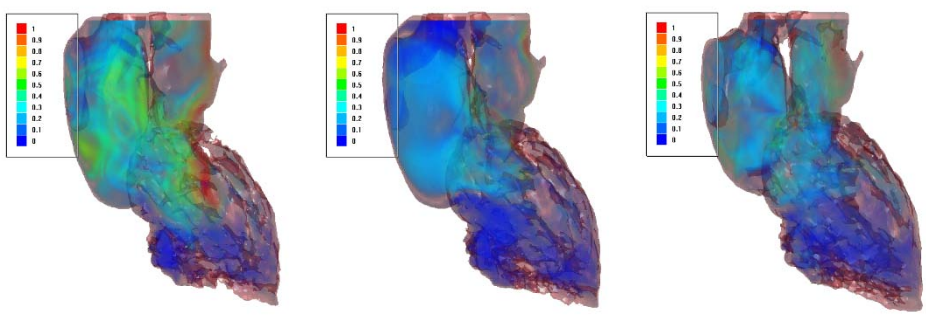

(d) t=0.6s (e) t= 0.8s (f) t=1.0s

Figure 15 Volume rendering of the velocity magnitude distribution

In Figure 13, the 4 sections are defined to show the pressure distribution in the flow field. We can notice that the pressure experience a large change in time, even at the specific time, there are still obvious pressure gradients between different sections. Moreover, the pressure variation nearby the outlet region is in agreement with the tendency in Figure 9(b). In the atrial systole period, the pressure inside is much bigger than diastole period, around the aorta area, where the pressure is relatively small due to the high flow velocity.

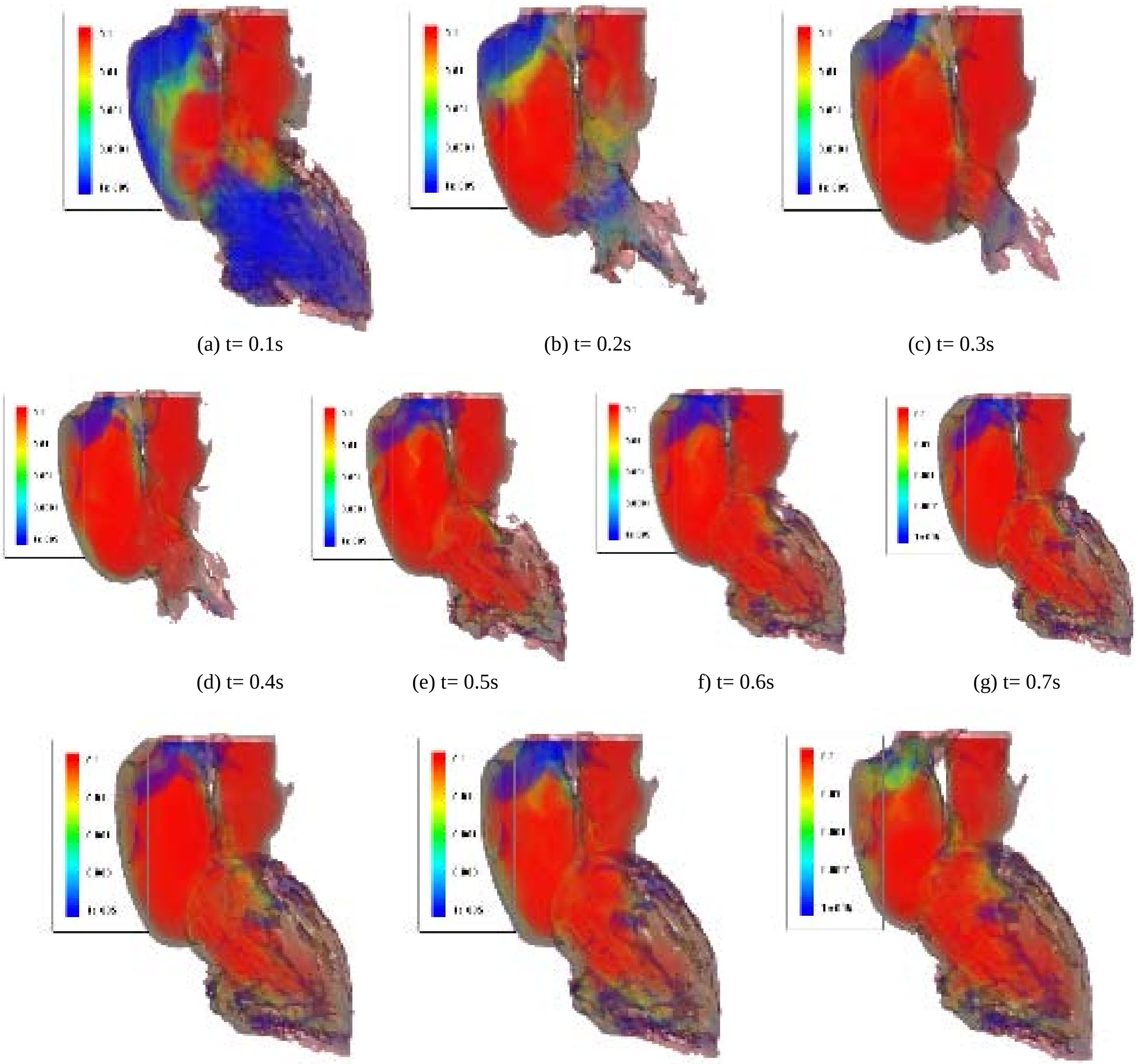

(a) t= 0.1s (b) t= 0.2s (c) t= 0.3s

(d) t= 0.4s (e) t= 0.5s f) t= 0.6s (g) t= 0.7s

(h) t= 0.8s (i) t= 0.9s (j) t= 1.0s

Figure 16 Volume rendering of turbulence viscosity

Similar to the pressure behaviour, the blood flow speed reaches its maximum, proximately at t=0.2s, which corresponds to the peak pressure in Figure 9 (b). In a cardiac cycle, the blood flow speed is extremely slow (see Figure 14 and Figure 15), where the magnitude is always ranging from 0 to 1m/s. The average velocity during systole is also bigger than during the diastole period, and the peak velocity at different stage is in agreement with the results found in the referenced literature [10].

Generally in the human body, the blood flow is laminar. However, under the conditions of high flow velocities, particularly in the ascending aorta, the laminar flow can be disrupted and thus becomes turbulent, as shown in Fig. 16. In a cardiac cycle, the turbulence viscosity in the aorta is always far bigger than the viscosity in laminar flow. Even in the most of the other heart parts, the blood flow behaves as the turbulent flow. Thus, the internal flow in human heart can be regarded as fully turbulent fluid flow.

IV. CONCLUSION

In this paper, a novel approach for simulating the blood flow applying the data from MRI/MRT scanners in the CFD tool FlowVision is presented. The Sub-Grid Geometry Resolution method for the mesh generation with the Euler approach is applied in order to take into account the moving walls of the living heart. The performed numerical simulations applying the FlowVision have made possible to get the pressure and velocity distributions of the blood flow inside the heart, as well as, these results have been analysed through the visualization methods integrated in FlowVision, being an essential part for this type of analysis enabling these flow fields to be shown with planar and volume rendering filtering techniques.

As this work present the very early research of heart modelling, the simulated internal flow didn’t involve the influence of cardiac valves, and this will be carried out in future work, which will focus on the FSI analysis, and further on to be combined with the electromagnetic prompting valves.

In general, this modelling and simulation methodology can be applied to solve similar flow phenomena, which are affected with the complex time-variant shape behaviour, as the authors recently performed for the MAAT project, where the flight of the Feeder airship has been simulated.

ACKNOWLEDGMENT

The presented work in this paper received a strong support from Capvidia and has found a common base with the European Commission FP7 MAAT project, when simulating the variable volume airship, and the authors gratefully acknowledge them.

REFERENCES

[1] A Kumar, “Changing trends of cardiovascular risk factors among Indians: a review of emerging risks,”Asian Pacific Journal of Tropical Biomedicine, 2014, 4(12): 1001-1008.

[2] Baskurt OK, Meiselman HJ,“Blood rheology and hemodynamics,” Seminars in Thrombosis and Haemostasis 29: 435–450.

[3] S. C. O. Noutchie, “Flow of a Newtonian fluid: The case of blood in large arteries,” Master of Science, University of South Africa, November 2005.

[4] David Rubenstein , Wei Yin, Mary D. Frame, “Biofluid Mechanics: An Introduction to Fluid Mechanics,” London: Elsevier, second edition 2015, pp. 466.

[5] Cheng Y, Oertel H, Schenkel T, “Fluid-structure coupled CFD simulation of the left ventricular flow during filling phase,” Annals of biomedical engineering, 2005, 33(5): 567-576.

[6] Baccani, B., F. Domenichini, G. Pedrizzetti, “Model and influence of mitral valve opening during the left ventricular filling,” J. Biomech. 36:355–361, 2003.

[7] Keber, R, “Computational fluid dynamics simulation of human left ventricular flow,” PhD Dissertation, University of Karlsruhe, Karlsruhe, 2003.

[8] Long, Q., R. Merrifield, G. Z. Yang, X. Y. Xu, P. J. Kilner, D. N. Firman, “The influence of inflow boundary conditions on intra left ventricle flow predictions,” J. Biomech. Eng. 125:922–927, 2003.

[9] Nakamura, M., S. Wada, T. Mikami, A. Kitabatake, T. Karino, “A computational fluid mechanical study on the effects of opening and closing of the mitral orifice on a transmitral flow velocity profile and an early diastolic intraventricular flow,” JSME Int. J. Ser. C – Mech. Syst. Mach. Elem. Manufact. 45:913–922, 2002.

[10] Wexler L, Bergel DH, Gabe IT, “Velocity of blood flow in normal human venae cavae,” Circulation Research, 1968, 23 (3): 349-359.

[11] Wilcox D. C. (1994),“Turbulence modeling for CFD,” DCW Industries, Inc., 460 p.

[12] Aksenov A, Dyadkin A, Pokhilko V. “Overcoming of Barrier between CAD and CFD by Modified Finite Volume Method,” Proc. 1998 ASME Pressure Vessels and Piping Division Conference, San Diego, ASME PVP-Vol. 377-2., 1998. pp. 79-86.